ELSEVIER

International Journal of Mass Spectrometry 210/211 (2001) 489–501

www.elsevier.com/locate/ijms

Benzonitrile assisted enolization of the acetone and acetamide radical cations: proton-transport catalysis versus an intermolecular $H^{+/\cdot}$ transfer mechanism

Moschoula A. Trikoupis[a], Peter C. Burgers[b], Paul J.A. Ruttink[c], Johan K. Terlouw[a,*]

[a]*Department of Chemistry, McMaster University, Hamilton, Ontario L8S 4M1, Canada*
[b]*Hercules European Research Center, Hercules B.V., P.O. Box 252, 3770 AG, Barneveld, The Netherlands*
[c]*Theoretical Chemistry Group, Department of Chemistry, University of Utrecht, Padualaan 14, 3584 CH Utrecht, The Netherlands*

Received 24 November 2000; accepted 9 February 2001

Abstract

The acetamide radical cation, $CH_3C(=O)NH_2^{\cdot +}$, can be induced to rearrange into its more stable enol isomer, $CH_2=C(OH)NH_2^{\cdot +}$, by an ion–molecule interaction with benzonitrile, $C_6H_5C{\equiv}N$, under conditions of chemical ionization. (This enolization does not occur unassisted because of a prohibitively high energy barrier: 26 kcal/mol, from a CBS-QB3 calculation.) The initially formed $[C_6H_5C{\equiv}N \cdots \text{acetamide}]^{\cdot +}$ adduct ion isomerizes to a stable hydrogen bridged radical cation $[C_6H_5C{\equiv}N \cdots H{-}O{-}C(NH_2){=}CH_2]^{\cdot +}$ en route to its dissociation into the enol ion. Multiple collision and deuterium labeling experiments on the acetamide/benzonitrile and the previously reported acetone/benzonitrile systems, indicate that the acetone ion enolizes by way of a base-catalyzed 1,3-proton shift ("proton-transport catalysis") but that a different mechanism must be operative in the acetamide system. Ab initio and density functional theory calculations at the PMP3//RHF/D95** and PMP3//B3LYP/D95** level of theory support a mechanism which can be described as a consecutive $H^+/H^{\cdot}$ transfer between the partners of the $[C_6H_5C{\equiv}N^{\cdot +} \cdots \text{acetamide}]$ encounter complex. The calculations provide a rationale for the observed isotope effects and lead to a tentative explanation for the differences in interaction of the title ions with benzonitrile. (Int J Mass Spectrom 210/211 (2001) 489–501) © 2001 Elsevier Science B.V.

Keywords: Proton-transport catalysis; Tandem mass spectrometry; Enolization; Dimer radical cation; Ab initio calculations; CBS-QB3, G2

1. Introduction

For years biochemists and chemists have been studying proton exchange in amides, peptides and proteins in solution [1]. This has also been the topic of several gas-phase studies [2] aimed at evaluating the number of sites that may be involved in proton transfer within a gaseous species and at differentiating isomers. Recently, a number of elegant experimental and theoretical studies [3] have reported mechanisms by which a gaseous conventional radical cation $[H{-}X{-}Y]^{\cdot +}$ isomerizes into its more stable distonic isomer $[X{-}Y{-}H]^{\cdot +}$ by way of interaction with a single solvent molecule B. One prominent example concerns $X{=}CH_2$ and $Y{=}OH$, that is the α-distonic

* Corresponding author. E-mail: terlouwj@mcmaster.ca

Dedicated to Professor Nico Nibbering on the occasion of his imminent retirement, in appreciation of his seminal contributions to the field of gas-phase ion chemistry.

PII S1387-3806(01)00412-2

ion $[CH_2OH_2]^{\cdot +}$. This ion is ~7 kcal/mol more stable than its isomer of conventional structure, $[CH_3OH]^{\cdot +}$, but the two isomers do not interconvert because the 1,2-H shift involved imposes a barrier of 26 kcal/mol. However a molecule of water (B) catalyzes this shift and promotes a smooth transformation of $[CH_3OH]^{\cdot +}$ into $[CH_2OH_2]^{\cdot +}$ [3b]. From detailed ab initio calculations [3c–f] it follows that O · H · O and C · H · O hydrogen-bridged radical cations play a prominent role in this transformation. In more general terms the "catalysis" has been proposed [3d] to take place when the proton affinity (PA) of the base B, lies between the PA of [X–Y] at X and Y, according to

$$B + [H–X–Y]^{\cdot +} \rightarrow B \cdots H^{+} \cdots [X–Y]^{\cdot} \rightarrow B \cdots H^{+} \cdots [Y–X]^{\cdot} \rightarrow B + [H–X–Y]^{\cdot +} \quad \text{Eq. (1)}$$

A similar mechanism has been proposed for the transport of methyl cations [4]. In a recent computational study, Radom and co-worker [3f], using the G2** and G2(ZPE=MP2) methods investigated the catalysis of proton and methyl cation transport reactions. For proton-transport catalysis it was shown that when PA[B] is intermediate, the barrier becomes negative relative to the separated reactants and products and the base successfully catalyzes the isomerization. If the PA of B is lower than the PA of $[X–Y]^{\cdot}$ at X, then formation of the first complex cannot take place. However, if the PA of B is higher than the PA of $[X–Y]^{\cdot}$ at Y, the complex initially formed dissociates into BH^{+} and $[X–Y]^{\cdot}$. The same holds true for methyl cation transfers but it is noted that the dipole moment of the base plays a significant role in the catalysis; the intermediate complexes formed are stabilized by strong electrostatic interactions when the base has a significant dipole moment.

This catalysis not only works for 1,2-H transfers [3], it also operates on 1,3-H transfers [5]. One example is the enolization of acetone radical cations [5b], which readily occurs when benzonitrile is used as the base. Further, in a recent Fourier transform ion cyclotron resonance study, Audier and co-workers [5c] demonstrated that acetone catalyzes the enolization of the acetophenone radical cation, $[C_6H_5C(=O)CH_3]^{\cdot +}$. This is an intriguing system where the catalyzed transfer follows a different route from the unimolecular isomerization: a 1,3-H transfer occurs rather than two 1,4-H shifts. In this context, it is of interest to note that some 20 years ago, Nibbering and co-workers [6] elegantly demonstrated that the loss of $CH_3^{\cdot}$ from *o*-hydroxybutyrophenone is preceded by an intramolecular proton-transport catalysis reaction involving the ortho OH group as the catalyst for the observed enol to keto isomerization.

Inspired by these findings we set out to examine the "single solvent molecule assisted" isomerization of ionized acetamide $[CH_3C(=O)NH_2]^{\cdot +}$ into its more stable enol form $[CH_2=C(OH)NH_2]^{\cdot +}$. We chose this system because preliminary considerations led us to believe that the acetamide ion would behave in much the same way as the acetone radical cation [5b]. That is, with benzonitrile the acetamide ion should also easily enolize via proton-transport catalysis. However, it quickly became clear, see below, that enolization of the acetamide ion proceeds via an entirely different mechanism.

2. Experimental and theoretical methods

The experiments were performed with the McMaster University VG Analytical (Manchester, UK) ZAB-R instrument of BE_1E_2 geometry (B, magnet; E, electric sector). Metastable ion (MI) mass spectra were recorded in the second field free region (2ffr); collision-induced dissociation (CID) mass spectra were recorded in the 2 and 3ffr using oxygen as collision gas (transmittance, T=70%). The CID mass spectra of the 2ffr metastable or collision-induced peaks were obtained in the 3ffr using O_2 as collision gas. For these experiments the maximum available accelerating voltage, 10 kV, was used. CID spectra of reference ions having a translational energy close to that of product ions resulting from (MI or CID) dissociations in the 2ffr, were also obtained in the 3ffr. Neutralization–reionization (NR) mass spectra were recorded using N,N-dimethylaniline as the reducing agent and oxygen gas for reionization. All spectra were recorded using a small PC-based data system developed by Mommers Technologies Inc. (Ottawa).

Table 1
CBS-QB3 and G2 derived enthalpies (298 K, kcal/mol) for ions and neutrals associated with the isomerization and dissociation of the acetamide radical cation

Species		CBS-QB3	G2	Expt.[a]
$CH_3C(=O)NH_2^{\cdot+}$	**1**$^{\cdot+}$	168.5	169	165
$CH_2=C(OH)NH_2^{\cdot+}$	**1a**$^{\cdot+}$	152	153	···
$CH_3C(OH)=NH^{\cdot+}$	**1b**$^{\cdot+}$	180	180	···
TS ($1^{\cdot+} \rightarrow 1a^{\cdot+}$)		194	···	···
TS ($1^{\cdot+} \rightarrow 1b^{\cdot+}$)		210.5	···	···
TS ($1a^{\cdot+} \rightarrow 1b^{\cdot+}$)		213.5	···	···
$CH_2NH_3^{\cdot+}$ + CO		176.5	176.5	175
$CH_3C{=}O^+$ + $NH_2^{\cdot}$		203	203	203.5
$NH_2C{=}O^+$ + $CH_3^{\cdot}$[b]		199.5	200	196
$CH_3C(OH)NH_2^+$		105	102.5	103
$^{\cdot}CH_2C(=O)NH_2$		−10	−10.5	···
$CH_3C(=O)NH^{\cdot}$[c]		3	···	···
$CH_3C(=O)NH_2$	**1**	−56.5	−58	−57
$CH_2=C(OH)NH_2$	**1a**	−31.5	−32	···
$CH_3C(OH)=NH$	**1b**	−42.5	−42.5	···

[a] See [12a].
[b] Using $\Delta H_f[NH_2C{=}O^+]$ = 161 kcal/mol, see [13c].
[c] This calculation suffered from a spin contamination ($<s^2>$ = 0.89).

Compounds were of research grade (Aldrich) and used without further purification. Acetamide-d_3 was synthesized on a small scale by reacting $CD_3C(=O)Cl$ with NH_3 whereas benzonitrile-d_5 was synthesized using the procedure described in [7].

Standard ab initio molecular orbital calculations were performed with the GAUSSIAN 98 [8] and GAMESS-UK [9] systems of programs. For all species associated with the unimolecular chemistry of the acetamide ion, standard CBS-QB3 [10] and G2 [11] procedures were followed to obtain the results presented in Table 1. Frequency calculations gave the correct number of negative eigenvalues for all minima and transition states reported. Unless otherwise stated, the spin contamination was acceptable, within 10% of 0.75.

3. Results and discussion

3.1. Unimolecular chemistry of the acetamide ion and its enol and iminol counterparts

The acetamide radical cation $CH_3C(=O)NH_2^{\cdot+}$, **1**$^{\cdot+}$, has two stable hydrogen shift isomers, the enol ion $CH_2=C(OH)NH_2^{\cdot+}$, **1a**$^{\cdot+}$ and the iminol ion $CH_3C(OH)=NH^{\cdot+}$, **1b**$^{\cdot+}$. For ions **1**$^{\cdot+}$ and **1a**$^{\cdot+}$, Schwarz and co-workers [2b], in an early ab initio study, found the enol ion to be more stable than its keto counterpart, by 16 kcal/mol. At this level of theory, MP3/6-31G(*d,p*)//HF/3-21G+ZPVE, we found the iminol ion **1b**$^{\cdot+}$ to lie higher in energy than both its enol and its keto counterpart, by 28 and 12 kcal/mol, respectively. These values agree remarkably well with those obtained from the more sophisticated G2 and CBS-QB3 procedures, see Table 1.

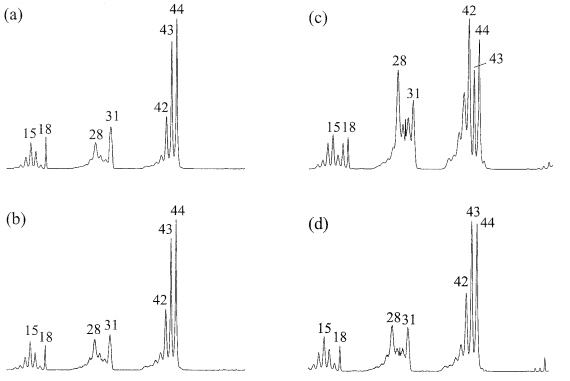

Fig. 1. 8 keV CID mass spectra of: (a) acetamide; (b) iminol of acetamide; (c) enol of acetamide; and (d) *m/z* 59 ions generated in the benzonitrile chemical ionization mass spectrum of acetamide.

From Table 1, it follows that the tautomeric ions are separated by high energy barriers. This is in line with the detailed experimental observations of Schwarz and co-workers [2b] who showed that the keto and enol ions **1**$^{\cdot+}$ and **1a**$^{\cdot+}$ have characteristically different MI and CID spectra. In brief, the MI spectrum of **1**$^{\cdot+}$ is dominated by a rearrangement ion at *m/z* 31, $CH_2NH_3^{\cdot+}$, whereas the enol ion **1a**$^{\cdot+}$ largely dissociates into *m/z* 44, $NH_2C{=}O^+$. A characteristic feature of the CID spectrum of **1a**$^{\cdot+}$, compare Fig. 1(a) and (c), is the prominent *m/z* 42 $CH_2{=}C{=}O^{\cdot+}$ ion, generated by loss of NH_3.

So far, no experimental observations have been reported on the iminol ion, $CH_3C(OH)=NH^{\cdot+}$, **1b**$^{\cdot+}$. Considering that ionized formamide's iminol counterpart, ionized formimidic acid, can cleanly be generated from N-formylhydrazone [2a], we decided to examine the N-acetyl-acetichydrazone **I**, as a precursor to **1b**$^{\cdot+}$. Indeed, the 70 eV electron ionization (EI) mass spectrum of **I** shows a prominent peak at *m/z* 59

which could correspond to iminol ions generated by way of in a McLafferty type rearrangement:

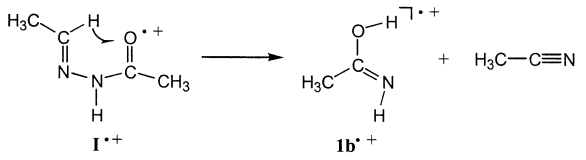

I$^{\cdot+}$ **1b**$^{\cdot+}$

EI ionization of N-hydroxymethylacetamide, **II**, also yields *m/z* 59 ions, which again could be ions **1b**$^{\cdot+}$ generated by loss of CH_2=O in a McLafferty type rearrangement:

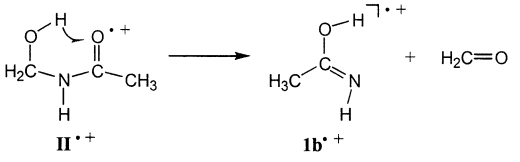

II$^{\cdot+}$ **1b**$^{\cdot+}$

The CID spectra of the *m/z* 59 ions from the above precursor molecules were obtained and found to be identical within experimental error, see Fig. 1(b) for a representative spectrum. However, this spectrum is also very close to that of the keto ion **1**$^{\cdot+}$, compare Fig. 1(a) and (b). This raises the question whether it is the keto ion which is generated in the previous dissociations. One rationalization would be that en route to the losses of $CH_3C{\equiv}N$ and CH_2=O, these neutral species lower the high barrier for the exothermic ketonization, see Table 1, of the incipient iminol ions by an intramolecular proton-transport catalysis process [12].

However, this is probably not the case since the closely similar MI spectra of the *m/z* 59 ions from the two precursor molecules are uniquely different from those of the keto and the enol isomers. These spectra are dominated by *m/z* 43 ($CH_3C{=}O^+$) and *m/z* 44 ($NH_2C{=}O^+$) ions of equal abundance. This is readily understandable considering the calculated energy level of transition state (TS) (**1b**$^{\cdot+}{\rightarrow}$**1**$^{\cdot+}$**)** vis à vis those of the dissociation products $CH_3C{=}O^+ + {}^{\cdot}NH_2$ and $NH_2C{=}O^+ + {}^{\cdot}CH_3$, see Table 1. The similarity between the CID spectra is therefore probably due to postcollisional isomerization of the iminol ion into energy-rich keto ions.

Thus, whereas enolization of the keto ions can easily be monitored by CID experiments, their iminolization cannot be detected. However, it is not expected that iminolization occurs in our chemical ionization type experiments, because the reaction is endothermic and associated with a high barrier, see Table 1.

3.2. Benzonitrile assisted enolization of ionized acetamide, experimental observations

As argued in Sec. 3.1, the unassisted enolization of the acetamide ion **1**$^{\cdot+}$ does not occur. However, the proton-transport catalysis criterion represented by Eq. (1) predicts that efficient enolization of ions **1**$^{\cdot+}$ should take place in an ion-molecule encounter complex with a neutral base whose PA lies between the PA of ${}^{\cdot}CH_2C(=O)NH_2$ at C and at O.

From the ΔH_f values for [${}^{\cdot}CH_2C(=O)NH_2$]=−10 kcal/mol (Table 1), [$CH_3C(=O)NH_2^{\cdot+}$]=165 kcal/mol [13a], [CH_2=$C(OH)NH_2^{\cdot+}$]=152 kcal/mol (Table 1) and [H^+]=366 kcal/mol [13a], the PA values for protonation of ${}^{\cdot}CH_2C(=O)NH_2$ at C and at O are estimated to be 191 and 204 kcal/mol, respectively.

Benzonitrile, a suitable base for the enolization of the acetone ion [5b], also appeared to be a candidate for the enolization of ionized acetamide: it has a PA, 196 kcal/mol [13b], that lies in the above mentioned range and it does not readily self-protonate (a process that is estimated to be endothermic by 7 kcal/mol) [14]. Further, benzonitrile and acetamide have similar IEs, 9.62 and 9.65 eV [13a], and substantial dipole moments, 4.2 and 3.8 Debye, respectively [15]. As a result, in our type of chemical ionization experiment, see below, the ion-molecule encounter complexes between benzonitrile and acetamide (AA), are likely to be of two types, viz. [$C_6H_5C{\equiv}N \cdots AA^{\cdot+}$] and [$C_6H_5C{\equiv}N^{\cdot+} \cdots AA$] which may interconvert by way of charge transfer (CT).

Benzonitrile, when introduced into the chemical ionization (CI) source to an indicated pressure of 6×10^{-5} Torr, shows little self-protonation: *m/z* 103 ($M^{\cdot+}$) : *m/z* 104 ($M+H^+$)=4. Other peaks observed in the spectrum include dissociation products of $M^{\cdot+}$ at *m/z* 76, 63, and 39, adducts of these ions and benzonitrile at *m/z* 179, 166, and 142 and a prominent proton bound dimer ion at

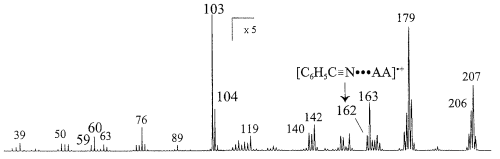

Fig. 2. CI mass spectrum of the benzonitrile/acetamide system.

m/z 207. In addition, a relatively intense peak is observed for the dimer radical cation at *m/z* 206. Peaks in the region *m/z* 54–61 were absent.

Next, a small amount of acetamide (AA) was introduced into the ion source and in the resulting spectrum, see Fig. 2, a relatively intense peak appeared at *m/z* 59 $[AA]^{\bullet+}$ in addition to a more intense *m/z* 60 $[AA+H]^+$; the latter is not unexpected since the self-protonation of acetamide and also that by benzonitrile are exothermic processes, by 15 and 3 kcal/mol, respectively [16]. Other peaks appeared at *m/z* 119, the proton bound dimer $[AA\cdots H\cdots AA]^+$, *m/z* 140, and *m/z* 163, the proton bound dimer $[C_6H_5C{\equiv}N\cdots H\cdots AA]^+$. Most importantly, a peak at *m/z* 162 corresponding to the $[C_6H_5C{\equiv}N\cdots$ "acetamide"$]^{\bullet+}$ ion also features in the spectrum.

The MI spectrum of the *m/z* 162 $[C_6H_5C{\equiv}N\cdots$ "acetamide"$]^{\bullet+}$ complex displays intense peaks at *m/z* 59 and 60 ($CH_3C(OH)NH_2^+$) and a minor signal at *m/z* 103, $[C_6H_5CN]^{\bullet+}$, see Fig. 4(a). The CID mass spectrum of these *m/z* 59 ions obtained from an tandem mass spectrometry (MS/MS/MS) experiment [17], see Fig. 3(d), reveals that they have the enol structure $\mathbf{1a}^{\bullet+}$. This experiment leaves no doubt that the original acetamide keto ion has been converted to its enol counterpart, compare Fig. 3(d) and (c).

The EI mass spectrum of Fig. 2 also displays a weak signal at *m/z* 118. From its MI and CID spectra it follows that these ions represent the acetamide dimer radical cation $[AA]_2^{\bullet+}$, in admixture with a benzonitrile derived adduct ion. Characteristic of the $[AA]_2^{\bullet+}$ component are prominent peaks at *m/z* 59 and 60 in the MI spectrum. Acetamide itself has a PA of 206 kcal/mol [13b] and it could therefore promote the enolization of the ionic component of the $[AA]_2^{\bullet+}$ complex. This is indeed the case: the *m/z* 59 ions generated from the metastable *m/z* 118 ions transmitted into the 3ffr yield a CID mass spectrum which is clearly that of the enol ion $\mathbf{1a}^{\bullet+}$. These matters will be discussed in a forthcoming article.

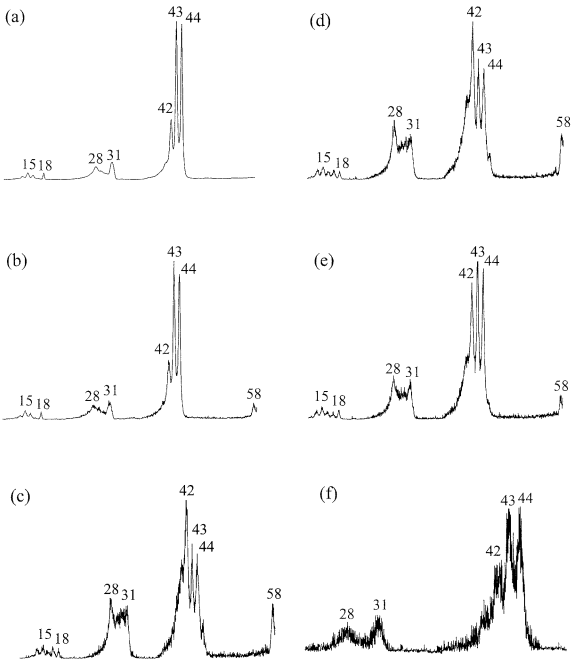

Fig. 3. 4 keV CID mass spectra of: (a) acetamide; (b) iminol of acetamide; (c) enol of acetamide; and (d) the metastably generated *m/z* 59 ions from the $[C_6H_5CN\cdots$ acetamide$]^{\bullet+}$ complex; (e) the collisionally formed *m/z* 59 ions from the $[C_6H_5CN\cdots$ acetamide$]^{\bullet+}$ complex; (f) the *m/z* 59 ions generated from NR of the *m/z* 162 ions.

In a previous study [5b] on the benzonitrile catalyzed enolization of the acetone ion, we had concluded that prior to its spontaneous or collision-induced dissociation, the initially formed $[C_6H_5C{\equiv}N\cdots$ acetone$]^{\bullet+}$ complex completely rearranges, by way of proton-transport catalysis, to the very stable hydrogen-bridged radical cation (HBRC), $[C_6H_5C{\equiv}N\cdots$ enol of acetone$]^{\bullet+}$. If the benzonitrile/acetamide system behaves in the same way, then, see Scheme 1, the initially formed $[C_6H_5C{\equiv}N\cdots$ acetamide$^{\bullet+}]$ complex ion $\mathbf{2a}^{\bullet+}$ will have completely rearranged to $[C_6H_5C{\equiv}N\cdots$ enol of acetamide$]^{\bullet+}$, $\mathbf{4}^{\bullet+}$, in the microsecond time-frame. Upon collisional activation, the complex ion will then uniquely yield *m/z* 59 ions having the enol ion structure $\mathbf{1a}^{\bullet+}$ as this is the energetically most favourable dissociation reaction of the HBRC $\mathbf{4}^{\bullet+}$.

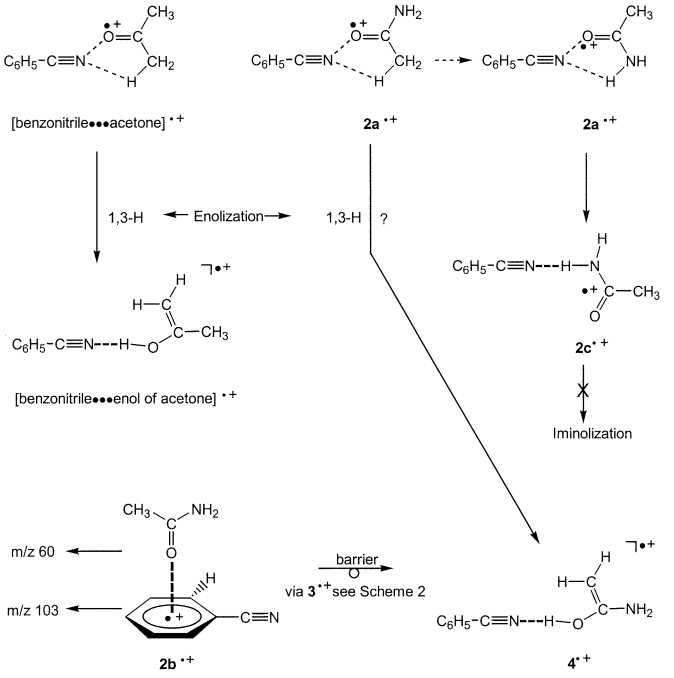

Scheme 1.

The actual experiment, however, points to a different scenario: in Fig. 3(e) is given the CID mass spectrum of the collisionally activated *m/z* 59 ions recorded in a MS/MS/MS experiment and it is clear that a mixture of enol and keto ions is produced, compare Fig. 3(e), (a), and (c). Thus, a significant fraction of the complex ions $\mathbf{2}^{\cdot+}$ has not rearranged into $\mathbf{4}^{\cdot+}$, even on the microsecond timeframe. In line with this, the *m/z* 59 ions present in the ion source have largely retained their keto identity, see Fig. 1(d).

To further probe the structure of the *m/z* 162 ion, its NR spectrum [18] was obtained. As expected for an ion–dipole complex, it was observed that a survivor signal is clearly absent and instead the spectrum displayed narrow peaks at *m/z* 59 and 103, indicative of the collisional ionization of the neutral(ized) components of the complex. The CID spectrum of the *m/z* 59 ions in the NR spectrum was obtained and, compare Fig. 3(f) and (a), these ions clearly represent the keto form, which further attests to the presence of un-rearranged precursor ions $\mathbf{2}^{\cdot+}$. By contrast, similar NR experiments on the $[C_6H_5C{\equiv}N \cdot \text{acetone}]^{\cdot+}$ complex [19] show that the neutral *m/z* 58 species consist solely of the enol form of acetone.

The internal energy of the precursor ions sampled by the different techniques falls in the order MI>CID>NR [20] and this is precisely what we observe: compare Fig. 3(d), (e), and (f). These results show that there is a significant barrier for the proton-transport catalysis putatively operative in the $[C_6H_5C{\equiv}N \cdots \text{acetamide}]^{\cdot+}$ complex, whereas no such barrier exists for the $[C_6H_5C{\equiv}N \cdots \text{acetone}]^{\cdot+}$ complex. In fact, the labeling experiments presented below indicate that proton-transport catalysis does not operate for the acetamide system and that an entirely different mechanism comes into play. In this context we further note, see Scheme 1, that acetamide's enolization is not necessarily associated with the route $\mathbf{2a}^{\cdot+} \rightarrow \mathbf{4}^{\cdot+}$. The pathway $\mathbf{2b}^{\cdot+} \rightarrow \mathbf{4}^{\cdot+}$ which starts from adduct ions in which the benzonitrile carries the charge may well be a more viable alternative, not least because $\mathbf{2a}^{\cdot+}$ type ions could collapse into the undoubtedly more stable HBRC $\mathbf{2c}^{\cdot+}$. This ion may serve as the precursor for a benzonitrile assisted

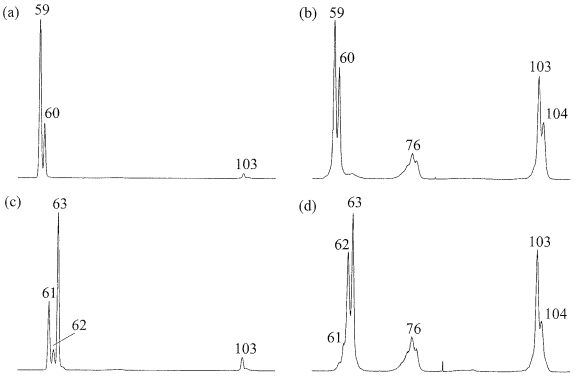

Fig. 4. MI mass spectra of: (a) the $[C_6H_5CN \cdots \text{ acetamide}]^{\cdot +}$ complex; (c) the $[C_6H_5CN \cdots \text{ acetamide-}d_3]^{\cdot +}$ complex; and their respective CID mass spectra (b) and (d).

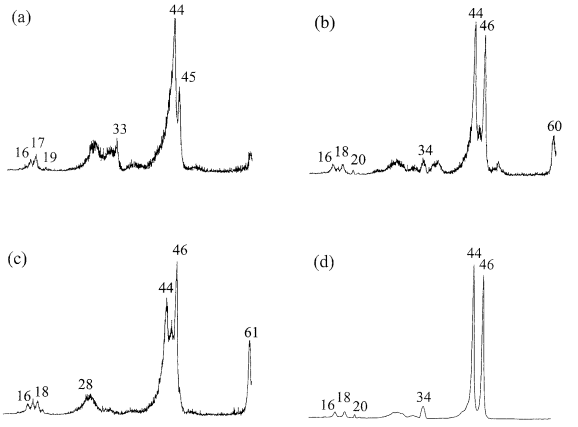

Fig. 5. CID mass spectra of the metastably generated: (a) *m/z* 61, (b) *m/z* 62, and (c) *m/z* 63 ions from the $[C_6H_5CN \cdots \text{ acetamide-}d_3]^{\cdot +}$ complex; (d) *m/z* 62 ions in the benzonitrile chemical ionization mass spectrum of acetamide-d_3, having 4 keV translational energy.

iminolization but, as pointed out previously, this process is not feasible on energetic grounds.

Analysis of the MI spectrum of the *m/z* 162 complex ion presented in Fig. 4(a) further underlines that the initially generated complex ions do not easily rearrange into the enolized complex ion $\mathbf{4}^{\cdot +}$. Formation of *m/z* 60 $[AA+H]^+$ ions from $\mathbf{2a}^{\cdot +}$ has a minimum energy requirement [21] which is slightly higher than that for the generation of $C_6H_5C{\equiv}NH^+$ (*m/z* 104)+$^{\cdot}CH_2C(=O)NH_2$, yet the latter reaction is not observed in the MI spectrum. Moreover, the even more energy demanding [21] dissociation into $C_6H_5C{\equiv}N^{\cdot +}+CH_3C(=O)NH_2$ is observed. These observations suggest that a sizeable fraction of the *m/z* 162 complex ions has retained the acetamide keto structure $\mathbf{2}^{\cdot +}$ and that, unlike the acetone case [5b], the benzonitrile assisted enolization of acetamide is still associated with a high-energy barrier.

3.3. D-labeled ions $[C_6H_5C{\equiv}N \cdots CD_3C(=O)NH_2]^{\cdot +}$ and $[C_6D_5C{\equiv}N \cdots CH_3C(=O)NH_2]^{\cdot +}$

To unravel the mechanism by which the enol ions are formed from the $[C_6H_5C{\equiv}N \cdots AA]^{\cdot +}$ ion, chemical ionization experiments using $CD_3C(=O)NH_2$ and $C_6H_5C{\equiv}N$ as well as $CH_3C(=O)NH_2$ and $C_6D_5C{\equiv}N$ were performed.

If an initially formed stable complex $\mathbf{2a/c}^{\cdot +}$ would rearrange to the HBRC $\mathbf{4}^{\cdot +}$ by way of proton-transport catalysis, then in the D-labeled isotopomer $[C_6H_5C{\equiv}N \cdots CD_3C(=O)NH_2]^{\cdot +}$ the complexed ion $CD_3C(=O)NH_2^{\cdot +}$, *m/z* 62, should rearrange to $CD_2{=}C(OD)NH_2^{\cdot +}$. An intense peak at *m/z* 62 is then expected in the MI spectrum of the complex which is presented in Fig. 4(c). From a comparison with the unlabeled result, see Fig. 4(a), it follows that this is not the case.

As mentioned earlier, the IEs of $C_6H_5C{\equiv}N$ and $CH_3C(=O)NH_2$ are virtually the same, so that a complex $\mathbf{2a/c}^{\cdot +}$ may interconvert with $\mathbf{2b}^{\cdot +}$ by way of charge transfer [22] or else ions $\mathbf{2b}^{\cdot +}$ may be generated directly. We propose that $C_6H_5C{\equiv}N^{\cdot +}$ in the latter complex donates a **proton** to its partner to produce $CH_3C(OH)NH_2^+$, *m/z* 60. As expected, this signal shifts to *m/z* 63 for the labeled ion. However, the peak at *m/z* 59 shifts to *m/z* 61 with the *m/z* 62 peak being much weaker. The CID mass spectrum of the metastably generated *m/z* 61 ions is shown in Fig. 5(a). This spectrum is dominated by loss of NH_3 and this reveals that the *m/z* 61 ions have the enol structure $CD_2{=}C(OH)NH_2^{\cdot +}$. Thus the transformation: $[C_6H_5C{\equiv}N + CD_3C(=O)NH_2]^{\cdot +} \rightarrow [C_6H_4DC{\equiv}N + CD_2{=}C(OH)NH_2]^{\cdot +}$ is established and this leads to the tentative proposal presented in Scheme 2.

The CID mass spectrum of the metastably generated *m/z* 62 ions is given in Fig. 5(b); it can be seen

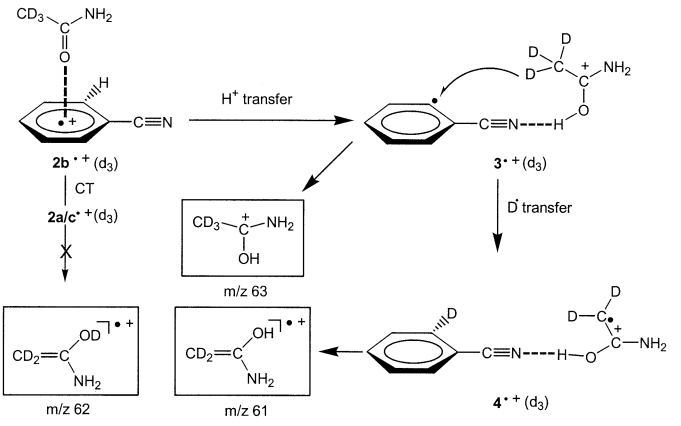

Scheme 2.

that losses of $NH_2^{\cdot}$ and $CD_3^{\cdot}$ are important processes and thus *m/z* 62 has the **keto** structure $CD_3C(=O)NH_2^{\cdot +}$. This ion, we propose, originates from dissociation of the un-rearranged complex ion $\mathbf{2a}^{\cdot +}$ (d_3) in Scheme 2. The results from Fig. 4(c) further reveal that an isotope effect (of magnitude 7) operates against the formation of *m/z* 61. From this we derive that the keto structure contributes only 3% to the unlabeled ions, which is entirely compatible with the CID mass spectrum of the metastably generated unlabeled ions, see previous discussions.

Thus, in the isomerization of the complex ion $\mathbf{2b}^{\cdot +}$ (d_3) a D transfer to the benzonitrile partner takes place, step $\mathbf{3}^{\cdot +} \rightarrow \mathbf{4}^{\cdot +}$ suggested in Scheme 2, and the above isotope effect indicates that this step may be rate determining.

Next, the complex $[C_6D_5C{\equiv}N \cdots CH_3C(=O)NH_2^{\cdot +}]$ was studied and its MI spectrum contains signals at *m/z* 59, 60, 61, and 108 with an intensity ratio of 45:100:55:25. CID experiments showed that *m/z* 59 represents the keto ion $CH_3C(=O)NH_2^{\cdot +}$, whereas *m/z* 60 is the enol ion $CH_2{=}C(OD)NH_2^{\cdot +}$. The signals at *m/z* 59 and *m/z* 108 will not suffer from an isotope effect and thus the reduced intensity of *m/z* 60 and 61 compared to *m/z* 59 and *m/z* 60 in the unlabelled spectrum, see Fig. 4(a), must be due to an isotope effect associated with the formation of $CH_2{=}C(OD)NH_2^{\cdot +}$ (*m/z* 60) and $CH_3C(OD)NH_2^{+}$ (*m/z* 61). Thus in Scheme 2, two isotope effects are operative, one for the abstraction of a hydrogen at the carbon atom from acetamide and one for the abstraction of a carbon hydrogen from benzonitrile. The order in which these processes occur remains "tentative," but they are both associated with relatively high-energy barriers of comparable magnitude.

Further support for the proposed mechanism comes from the CID mass spectra presented in Fig. 4(b) and (d). In the CID spectrum of the unlabeled complex, Fig. 4(b), additional peaks are present compared to its MI spectrum, notably *m/z* 104, protonated benzonitrile, $C_6H_5C{\equiv}NH^+$. Surprisingly, for the CD_3 labeled species, see Fig. 4(d), this signal does **not** shift to *m/z* 105, but remains at *m/z* 104 and thus upon collisional activation, $CD_3C(=O)NH_2^{\cdot +}$ donates an H, not a D, to benzonitrile, i.e.

$$[C_6H_5C{\equiv}N \cdots CD_3C(=O)NH_2^{\cdot}] \quad \mathbf{2a}^{\cdot +}\ (d_3)$$
$$\not\longrightarrow C_6H_5C{\equiv}ND^+ + {}^{\cdot}CD_2{=}C(OH)NH_2$$

but

$$[C_6H_5C{\equiv}N \cdots H_2NC(=O)CD_3^{\cdot}] \quad \mathbf{2c}^{\cdot +}\ (d_3)$$
$$\longrightarrow C_6H_5C{\equiv}NH^+ + {}^{\cdot}HNC(=O)CD_3$$

Thus ionized acetamide does **not** donate a carbon proton to the benzonitrile moiety, not even upon collisional activation. This despite the fact that a D^+ transfer is less endothermic than a H^+ transfer, by 13

kcal/mol, see Table 1. In contrast, in the $[C_6H_5C{\equiv}N \cdots \text{acetone}^{\cdot +}]$ complex a carbon proton is readily transferred to the benzonitrile moiety [5b].

These observations may well indicate that the encounter complex $\mathbf{2a}^{\cdot +}$ readily adopts the structure of the HBRC $\mathbf{2c}^{\cdot +}$ depicted in Scheme 1, as suggested previously.

4. Theoretical calculations

As mentioned in Sec. 3.3, in the initially formed complex $[C_6H_5C{\equiv}N \cdots AA]^{\cdot +}$, the charge will be on the benzonitrile moiety, see ion $\mathbf{2b}^{\cdot +}$ in Scheme 1. Charge transfer may furnish the complex $\mathbf{2a}^{\cdot +}$. Exploratory calculations indicated that if ionized acetamide and neutral benzonitrile meet to form such a complex, proton transfer from the carbon atom of ionized acetamide to benzonitrile would be associated with a large barrier but due to computational difficulties, the exact level of the transition state could not be assessed. Instead, we noted that ions of the type $\mathbf{2a}^{\cdot +}$ readily collapsed into the stable HBRC $\mathbf{2c}^{\cdot +}$, see Scheme 1.

However, when the charge is on the benzonitrile moiety, proton transfer in ion $\mathbf{2b}^{\cdot +}$ can yield the complex $[C_6H_4C{\equiv}N \cdots CH_3C(OH)NH_2^+]$, $\mathbf{3}^{\cdot +}$, where acetamide becomes protonated. If this complex lies in a sufficiently deep well a hydrogen **atom** transfer from the carbon atom of $CH_3C(OH)NH_2^+$ to $C_6H_4C{\equiv}N^{\cdot}$ might be possible leading to the HBRC $\mathbf{4}^{\cdot +}$ which then dissociates to $CH_2{=}C(OH)NH_2^{\cdot +}$ as observed. The labeling experiments discussed previously, indicate that the transition states $\mathbf{2b}^{\cdot +} \rightarrow \mathbf{3}^{\cdot +}$ and $\mathbf{3}^{\cdot +} \rightarrow \mathbf{4}^{\cdot +}$ should be relatively high and of comparable magnitude.

The calculations were started with restricted Hartree-Fock/double zeta polarization (RHF/DZP) geometry optimizations of various ions, transition states, and dissociation products depicted in Scheme 4, see also Scheme 1 and 2. Detailed geometries are only presented for the transition states, see Scheme 3: for all other species they are available upon request from the authors. All stationary points were checked for the correct number of imaginary frequencies. The transition from ion $\mathbf{2c}^{\cdot +}$ to ion $\mathbf{2b}^{\cdot +}$ appears to be a crossing: the charge is either located on the benzene ring or on the acetamide moiety. This holds for all levels of calculation used [RHF, unrestricted Hartree-Fock, and fourth-order Møller-Plesset (MP4)]. The minimum energy crossing point was determined using Morokuma's method [23] and single point calculations were performed with both choices of charge localization. The resulting energies are slightly different due to different electronic correlation effects for the two representations of the ground state in the crossing geometry.

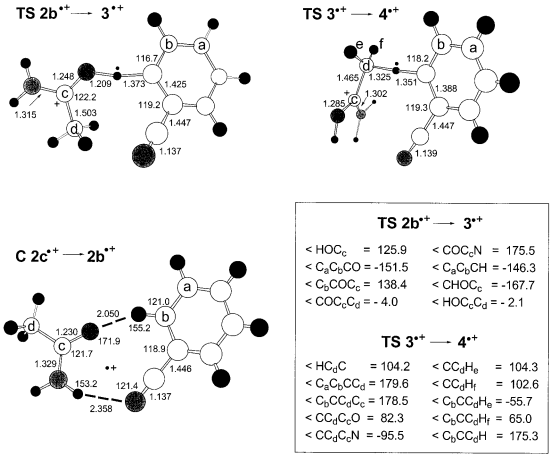

Scheme 3.

Single point UMP2/D95** calculations for the geometries found, showed that several ions suffer from a large spin contamination. This is especially true if the radical character is localized on the benzene ring, e.g. the $C_6H_4C{\equiv}N^{\cdot}$ radical has $\langle s^2 \rangle = 1.47$. In this model TS $\mathbf{2b}^{\cdot +} \rightarrow \mathbf{3}^{\cdot +}$ and TS $\mathbf{3}^{\cdot +} \rightarrow \mathbf{4}^{\cdot +}$ (also highly spin contaminated) turn out to lie 10 and 16 kcal/mol, respectively, above our anchor point, $C_6H_5C{\equiv}N + CH_3C(=O)NH_2^{\cdot +}$. This clearly is incompatible with the experimental observations. Therefore the UMP2 method was deemed unsuitable to obtain better geometries and the RHF geometries were used in all other ab initio calculations. To check whether this defect persists in the next higher orders of perturbation theory, UMP4SDTQ calculations were performed for the two transition states. Unfortunately, this does not significantly improve the results, TS

Table 2
Energies of TS $\mathbf{2b}^{\cdot+} \rightarrow \mathbf{3}^{\cdot+}$ and TS $\mathbf{3}^{\cdot+} \rightarrow \mathbf{4}^{\cdot+}$ (in kcal/mol) relative to the anchor point, $CH_3C(=O)NH_2^+ + C_6H_5C{\equiv}N$, for various theoretical models

Model	TS $\mathbf{2b}^{\cdot+} \rightarrow \mathbf{3}^{\cdot+}$	TS $\mathbf{3}^{\cdot+} \rightarrow \mathbf{4}^{\cdot+}$
RHF	18	23
UMP2	10	16
UMP3	9	14
UMP4SDQ	4	9
UMP4SDTQ	6	11
PMP2-O[a]	−3	−10
PMP2[b]	−1	−2
PMP3[b]	1	0
PMP4[b]	−3	−4

[a] Only the quartet (s = 3/2) component is projected out.
[b] Components with s = 3/2, 5/2, 7/2, and 9/2 are projected out.

$\mathbf{3}^{\cdot+} \rightarrow \mathbf{4}^{\cdot+}$ still lies 11 kcal/mol above the anchor point. Better results are, however, obtained if the spin-projected energies are used. The UMP2 calculation also yields PMP2-O energies, where only the next higher spin component (the quartet in our case) is projected out. This yields a dramatic lowering of the relative energy of TS $\mathbf{3}^{\cdot+} \rightarrow \mathbf{4}^{\cdot+}$: it now lies 10 kcal/mol **below** the anchor point. Further improvements may be expected by going to higher orders. This yields the results given in Table 2.

The results in Table 2 show that projecting out the quartet component has a large effect, but it still does not remove the spin contamination sufficiently. Although the annihilation of the higher components is still not complete in the PMPn calculations, a detailed inspection of the output shows that the results have converged to within 0.5 kcal/mol, which is quite satisfactory considering the other inaccuracies still present. To obtain PMP4 results full MP4 calculations have to be performed, i.e. calculations including the triple excitations. Such calculations appear to be very time consuming for a system of this size and complexity (the triples take ~95% of the CPU time). We therefore decided to restrict ourselves in our computational analysis of the present system to the MP4SDQ level of theory needed to obtain the PMP3 energies.

The above results were obtained using RHF optimized geometries. Since the RHF energies appear not to be very useful, we thought it worthwhile to try the density functional theory method for optimizing geometries. For this purpose the B3LYP parameterization was used. The Becke-style 3 parameter using the Lee-Yang-Parr correlation functional (B3LYP) results do not suffer from the spin contamination problem: the largest $\langle s^2 \rangle$ value is 0.77 (for $C_6H_4C{\equiv}N^{\cdot}$). The crossing situation for the $\mathbf{2c}^{\cdot+} \rightarrow \mathbf{2b}^{\cdot+}$ transition persists even in the B3LYP calculation which tends to delocalize the charge. The resulting geometries were again used for MP4SDQ single point calculations. The energies obtained from these PMP3//RHF/D95** and PMP3//B3LYP/D95** calculations are presented in Table 3.

The B3LYP energies appear to deviate significantly from the ab initio results, particularly for the transition states, whose relative energies are 13 and 17 kcal/mol below the ab initio results. Also, for $\mathbf{2b}^{\cdot+}$ the B3LYP method yields E(rel) = −27 kcal/mol, whereas the PMP3//RHF calculation yields E(rel) = −13 kcal/mol. It is also noteworthy that one of the two possible B3LYP charge distributions in the crossing geometry is delocalized over both moieties, even though they are far apart.

Although some of the B3LYP geometries also differ considerably from their RHF counterparts, the final (PMP3) relative energies, see Table 3 and the energy level diagrams of Scheme 4, are rather close. However, there is one notable exception and this concerns, see Scheme 4, TS $\mathbf{2c}^{\cdot+} \rightarrow \mathbf{2b}^{\cdot+}$ which is comparable in energy with **TS** $\mathbf{3}^{\cdot+} \rightarrow \mathbf{4}^{\cdot+}$ in the calculation based on RHF geometries but lower in the B3LYP based model. We note, see below, that the RHF geometries yield results, which are in good agreement with the experimental observations and surmise that the B3LYP calculation underestimates the height of this TS. We further note that both computational approaches satisfactorily reproduce the position of the various dissociation levels: e.g. the energy difference between $AA^{\cdot+}$ ($\mathbf{1}^{\cdot+}$) and $AAE^{\cdot+}$ ($\mathbf{1a}^{\cdot+}$) in Scheme 4, 16–17 kcal/mol, agrees quite well with the CBS-QB3 and G2 derived values, 16 kcal/mol, presented in Table 1. Moreover, the marginal energy difference between $BN^{\cdot+}$ + AA and the anchor point $AA^{\cdot+}$ + BN is in keeping with the

Table 3
Ab initio energies for the acetamide/benzonitrile system; electronic energies are in Hartrees and ZPEs in kcal/mol; data in parentheses are without ZPE contribution

	RHF	ZPE (*0.9)	*E*(rel)	PMP3/RHF	*E*(rel)	B3LYP	*E*(rel)	PMP3/B3LYP	*E*(rel)	Expt.[a] 298 K	$<s^2>$[b]
1	−208.031 03	44.4		−208.664 87	1.9	−209.263 97		−208.666 11			0
1 + $BN^{\cdot+}$	−530.196 55	103.1	14.9	−531.873 67		−533.451 00	−3.0	−531.878 27	1.1	0	
$BN^{\cdot+}$	−322.165 52	58.7		−323.208 80		−324.187 03		−323.212 16			0.966
$\mathbf{1}^{\cdot+}$[c]	−207.715 94		(10.7)	−208.312 01	(9.2)	−208.907 84	(6.0)	−208.315 42	(7.3)		0.763
$\mathbf{1}^{\cdot+}$	−207.733 02	44.8		−208.326 66		−208.917 33		−208.327 09			0.760
$\mathbf{1}^{\cdot+}$ + BN	−530.222 79	104.7	0	−531.879 49	0	−533.448 88	0	−531.882 81	0	0	
BN	−322.489 77	59.9		−323.552 83		−324.531 55		−323.555 72			0
BN + $\mathbf{1a}^{\cdot+}$	−530.238 53	104.6	−10	−531.905 19	−16.2	−533.475 56	−16.8	−531.909 84	−17.1		
$\mathbf{1a}^{\cdot+}$	−207.748 76	44.7		−208.352 36		−208.944 01		−208.354 12			0.770
$AA^{\cdot}(C)$[d]	−207.383 17	35.9		−207.985 40		−209.579 22		−207.988 19			0.766
$AA^{\cdot}(C)$ + BNH^{+}	−530.197 77	102.5	13.5	−531.860 76		−533.438 25	4.6	−531.866 07	8.4		
BNH^{+}	−322.814 60	66.6		−323.875 57		−323.859 03		−323.877 88			0
BNH^{+} $AA^{\cdot}(N)$	−530.212 83	102.8	4.4	−531.879 13	−1.7	−533.456 80	−6.9	−531.883 25	−1.6		
$AA^{\cdot}(N)$[d]	−207.398 23	36.2		−208.003 56		−208.597 77		−208.005 37			0.783
AAH^{+}	−208.383 71	53.1		−209.015 71		−209.610 89		−209.015 71			0
AAH^{+} + $BN^{\cdot}$	−530.216 50	105.4	4.6	−531.876 81	−1.1	−533.450 92	−0.7	−531.877 80	−2.5	−3[e]	
$BN^{\cdot}$	−321.832 79	52.3		−322.861 10		−323.840 03		−322.86 09			1.472
$\mathbf{2c}^{\cdot+}$	−530.261 11	105.8	−22.9	−531.921 51	−25.3	−533.491 40	−25.6	−531.924 75	−25.2		0.735
C $\mathbf{2c}^{\cdot+}$ − $\mathbf{2b}^{\cdot+}$	−530.223 81		(0.6)	−531.888 41	(−5.6)	−533.471 75	(−14.4)	−531.889 05	(−3.9)		0.762
C $\mathbf{2c}^{\cdot+}$ − $\mathbf{2b}^{\cdot+}$	−530.223 81		(0.6)	−531.898 27	(−11.8)	−533.471 75	(14.4)	−531.905 49	(−12.3)		0.978
2b	−530.226 57	104.3	−2.8	−531.901 92	−13.0	−533.492 36	−26.7	−531.903 52	−12.4		0.992
TS $\mathbf{2b}^{\cdot+} \rightarrow \mathbf{3}^{\cdot+}$	−530.189 71	101.9	18.0	−531.873 67	0.8	−533.463 66	−12.1	−531.872 50	−9.3		1.169
$\mathbf{3}^{\cdot+}$	−530.256 72	106.3	−19.7	−531.921 32	−24.6	−533.500 86	−31.0	−531.925 89	−25.3		1.408
TS $\mathbf{3}^{\cdot+} \rightarrow \mathbf{4}^{\cdot+}$	−530.183 82	102.9	22.7	−531.876 85	−0.2	−533.456 82	−6.9	−531.878 92	−4.3		1.434
$\mathbf{4}^{\cdot+}$	−530.280 25	105.7	−35.1	−531.949 87	−43.3	−533.524 41	−46.5	−531.953 52	−43.5		0.764

[a] See [13].
[b] In the large basis UHF calculation.
[c] Vertical ionization: calculated using the geometry of neutral acetamide. The relative energies are calculated from the electronic energies of this ion + neutral benzonitrile.
[d] $AA^{\cdot}(C) \rightarrow {}^{\cdot}CH_2C(=O)NH_2$, $AA^{\cdot}(N) \rightarrow CH_3C(=O)NH^{\cdot}$.
[e] ΔH_f ($BN^{\cdot}$) = 111 kcal/mol from [5b].

experimental observation that the IEs of AA and BN are virtually the same.

Using Scheme 4 as a guide, we propose that the reaction starts with either complex $\mathbf{2c}^{\cdot+}$ or $\mathbf{2b}^{\cdot+}$. Complex $\mathbf{2c}^{\cdot+}$ is a HBRC whose stabilization energy (SE) can be estimated from the empirical relationship SE=23.2−0.25ΔPA (kcal/mol) [24], where ΔPA is the difference in proton affinity between benzonitrile (196 kcal/mol) and the radical $CH_3C(=O)NH^{\cdot}$(206 kcal/mol, Table 1). We then obtain SE=21 kcal/mol, compared to 25 kcal/mol derived computationally, see Scheme 4.

Charge transfer may lead to complex $\mathbf{2b}^{\cdot+}$ where the acetamide neutral lies perpendicular to the plane of the benzonitrile ion. Proton transfer from the benzonitrile to acetamide is only possible if the benzonitrile and acetamide components lie in the same plane, TS $\mathbf{2b}^{\cdot+} \rightarrow \mathbf{3}^{\cdot+}$ in Scheme 3. The resulting complex $\mathbf{3}^{\cdot+}$ can be viewed as protonated acetamide interacting with the $C_6H_4C{\equiv}N^{\cdot}$ radical. This radical can then rotate until a TS is reached, TS $\mathbf{3}^{\cdot+} \rightarrow \mathbf{4}^{\cdot+}$, where a H atom lies midway between the benzonitrile and the enol of acetamide moiety, see Scheme 3. This yields the very stable HBRC $\mathbf{4}^{\cdot+}$ which represents the ionized enol

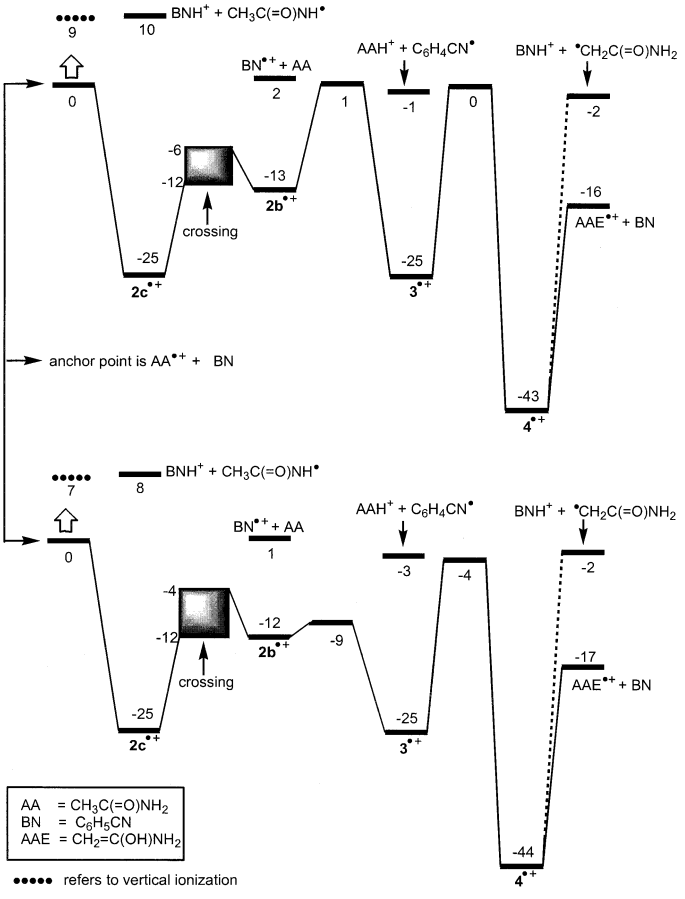

Scheme 4.

of acetamide interacting with the benzonitrile dipole. This ion then dissociates to $CH_2{=}C(OH)NH_2^{\cdot+}$, as observed.

The computationally derived scenario for the interactions and dissociations of the $[C_6H_5C{\equiv}N\cdots AA]^{\cdot+}$ system in Scheme 4, supports the tentative mechanistic proposal of Scheme 3 and the associated experimental observations. First, complex $\mathbf{2c}^{\cdot+}$ accounts for the formation of the acetamide ion, $\mathbf{1}^{\cdot+}$, in the metastable time-frame and it also, upon activation, generates $C_6H_5C{\equiv}NH^+ + CH_3C(=O)NH^{\cdot}$, as observed. Complex $\mathbf{2b}^{\cdot+}$ can generate $C_6H_5C{\equiv}N^{\cdot+}$ metastably, whereas ion $\mathbf{3}^{\cdot+}$ may serve as the precursor for $CH_3C(OH)NH_2^+$. In the RHF based calculation, the transition $\mathbf{2b}^{\cdot+} \rightarrow \mathbf{3}^{\cdot+}$ lies sufficiently high to account for the observed isotope effect in the complex ion $[C_6D_5C{\equiv}N\cdots CH_3C(=O)NH_2]^{\cdot+}$. Finally, complex $\mathbf{4}^{\cdot+}$ yields the enol of acetamide ion, $\mathbf{1a}^{\cdot+}$, and its formation from $\mathbf{3}^{\cdot+}$ is associated with a barrier of such a magnitude that it could account for the observed isotope effect in the dissociation of the complex ion $[C_6H_5C{\equiv}N\cdots CD_3C(=O)NH_2]^{\cdot+}$. The stabilization energy of the HBRC $\mathbf{4}^{\cdot+}$ may be estimated from the empirical relationship SE=30.0−0.26PA (kcal/mol) [24]: SE=28 kcal/mol which compares well with the computationally derived value of 27 kcal/mol.

5. Conclusions

The acetamide radical cation $CH_3C(=O)NH_2^{\cdot+}$, $\mathbf{1}^{\cdot+}$, is separated from its more stable enol isomer

CH_2=C(OH)$NH_2^{\cdot+}$, **1a**$^{\cdot+}$, by a large barrier (26 kcal/mol) which prevents its unimolecular enolization. However, this barrier can be lowered sufficiently by interaction with an appropriate neutral molecule, such as benzonitrile, for the enolization to occur. Under conditions of chemical ionization the [$C_6H_5C{\equiv}N \cdots$ acetamide]$^{\cdot+}$ dimer radical cation is readily formed which rearranges to a [$C_6H_5C{\equiv}N \cdots$ "enol of acetamide"] complex. Analysis of the behaviour of labeled ions, and comparative experiments with [$C_6H_5C{\equiv}N \cdots$ acetone]$^{\cdot+}$ adduct ions, demonstrate that this isomerization does not occur by way of proton-transport catalysis, but rather by an intermolecular $H^+/H^{\cdot}$ transfer mechanism. In the initial [$C_6H_5C{\equiv}N^{\cdot+} \cdots$ acetamide] complex, benzonitrile, acting as an acid and not a base, transfers a proton to the carbonyl oxygen. In the next transformation a hydrogen atom is donated back to the $C_6H_5C{\equiv}N$ moiety, leading to the hydrogen-bridged radical cation [$C_6H_5C{\equiv}N \cdots H{-}O{-}C(NH_2){=}CH_2]^{\cdot+}$, **4**$^{\cdot+}$, which can dissociate into the enol ion **1a**$^{\cdot+}$ and benzonitrile. Theory and experiment agree that both H transfers are associated with fairly high-energy barriers.

In support of our mechanistic proposal, we note that if a "base" is used whose ionization energy is considerably higher than that of the acetamide, that enolization does not take effect. For example, acrylonitrile has an IE of 10.9 eV [11a], a PA of 190 kcal/mol [11b] and a dipole moment of 3.9 Debye [14] but its interaction with acetamide leads to complexes in which the acetamide moiety retains its keto structure.

Finally, we note that the reason why the proton-transport catalysis in the [$C_6H_5C{\equiv}N \cdots$ acetone]$^{\cdot+}$ encounter complex does not feature in the [$C_6H_5C{\equiv}N \cdots$ acetamide]$^{\cdot+}$ ion may find its explanation in the following two differences between the systems. First, as pointed out in the preceding sections the initial encounter complex **2a**$^{\cdot+}$ in Scheme 1, may easily collapse into the more stable but unreactive HBRC **2c**$^{\cdot+}$, an option not open to the [$C_6H_5C{\equiv}N \cdots$ acetone$^{\cdot+}$] ion. Second, and perhaps more importantly, in the case of the acetamide system, the transfromation **2a**$^{\cdot+} \rightarrow$ **4**$^{\cdot+}$ may be associated with a large barrier. Thus, when in **2a**$^{\cdot+}$ a proton is shifted from the ionized acetamide carbon to the benzonitrile nitrogen, the dipole vector of the incipient $^{\cdot}CH_2{-}C(=O)NH_2$ radical may point in the wrong direction leading to ion–dipole repulsion.

Acknowledgements

Two of the authors (J.K.T. and M.A.T.) thank the Natural Sciences and Engineering Research Council of Canada (NSERC) for financial support. Stimulating discussions with Professor H.-F. Grützmacher and Professor N.M.M. Nibbering are much appreciated. The authors would like to thank Lisa N. Heydorn for synthesizing the benzonitrile-d_5 sample.

References

[1] C.L. Perrin, Acc. Chem. Res. 22 (1989) 268.
[2] (a) G.A. McGibbon, P.C. Burgers, J.K. Terlouw, Int. J. Mass Spectrom. Ion Processes 136 (1994) 191 and references cited therein; (b) T. Drewello, N. Heinrich, W.P.M. Maas, N.M.M. Nibbering, T. Weiske, H. Schwarz, J. Am. Chem. Soc. 109 (1987) 4810.
[3] (a) P. Mourgues, H.-E. Audier, D. Leblanc, S. Hammerum, Org. Mass Spectrom. 28 (1993) 1098; (b) H.-E. Audier, D. Leblanc, P. Mourgues, T.B. McMahon, S. Hammerum, J. Chem. Soc. Commun. (1994) 2329; (c) J.W. Gauld, H.-E. Audier, J. Fossey, L. Radom, J. Am. Chem. Soc. 118 (1996) 6299; (d) J.W. Gauld, L. Radom, ibid. 119 (1997) 9831; (e) A.J. Chalk, L. Radom, ibid. 119 (1997) 7573; (f) A.J. Chalk, L. Radom, ibid. 121 (1999) 1574; (g) M.A. Trikoupis, D.J. Lavorato, J.K. Terlouw, P.J.A. Ruttink, P.C. Burgers, Eur. Mass Spectrom 5 (1999) 431; (h) for an early review see: D.K. Bohme, Int. J. Mass Spectrom. Ion Processes 115 (1992) 95.
[4] V. Baranov, S. Petrie, D.K. Bohme, J. Am. Chem. Soc. 118 (1996) 4500; see also A. Cunje, C.F. Rodriquez, D.K. Bohme, A.C. Hopkinson, J. Phys. Chem. A 102 (1998) 478.
[5] (a) G. Van der Rest, P. Mourgues, J. Tortajada, H.-E. Audier, Int. J. Mass Spectrom. 179/180 (1998) 293, and references cited therein; (b) M.A. Trikoupis, P.C. Burgers, J.K. Terlouw, J. Am. Chem. Soc. 120 (1998) 12131; (c) J. Chamot-Rooke, G. Van der Rest, P. Mourgues, H.-E. Audier, Int. J. Mass Spectrom. 195/196 (2000) 385; (d) A. Nixdorf, H.-F. Grützmacher, J. Am. Chem. Soc. 119 (1997) 6544.
[6] T.A. Molenaar-Langeveld, N.M.M. Nibbering, R.P. Morgan, J.H. Beynon, Org. Mass Spectrom. 13 (1978) 172.
[7] E.C. Taylor, H.W. Altland, R.H. Danforth, G. McGillivray, J. Am. Chem. Soc. 92 (1970) 3520.
[8] GAUSSIAN 98, revision A.7, M.J. Frisch, G.W. Trucks, H.B. Schlegel, G.E. Scuseria, M.A. Robb, J.R. Cheeseman, V.G. Zarzewski, J.A. Montgomery Jr., R.E. Stratmann, J.C. Burant, S. Dapprich, J.M. Millam, A.D. Daniels, K.N. Kudin, M.C.

Strain, O. Farkas, J. Tomasi, V. Barone, M. Cossi, R. Cammi, B. Mennucci, C. Pomelli, C. Adamo. S. Clifford, J. Ochterski, G.A. Petersson, P.Y. Ayala, Q. Cui, K. Morokuma, D.K. Malick, A.D. Rabuck, K. Raghavachari, J.B. Foresman, J. Cioslowski, J.V. Ortiz, A.G. Baboul, B.B. Stefanov, G. Liu, A. Liashenko, P. Piskorz, I. Komaromi, R. Gomperts, R.L. Martin, D.J. Fox, T. Keith, M.A. Al-Laham, C.Y. Peng, A. Nanayakkara, C. Gonzalez, M. Challacombe, P.M.W. Gill, B. Johnson, W. Chen, M.W. Wong, J.L. Andres, C. Gonzalez, M. Head-Gordon, E.S. Replogle, J.A. Pople, Gaussian Inc., Pittsburgh, PA, 1998.

[9] (a) M. Dupuis, D. Spangler, J. Wendolowski, NRCC Software Catalogue 1 Program No. QG01, GAMESS (1980); (b) M. Guest, J. Kendrick, GAMESS User Manual, An Introductory Guide, CCP/86/1, Daresbury Laboratories, 1986.

[10] (a) J.A. Montgomery Jr., M.J. Frisch, J.W. Ochterski, G.A. Petersson, J. Chem. Phys. 112 (2000) 6532; (b) 110 (1999) 2822.

[11] L.A. Curtiss, K. Raghavachari, G.W. Trucks, J.A. Pople, J. Chem. Phys. 94 (1991) 7221.

[12] For a brief review see: J.K. Terlouw, Proton-Transport Catalysis in Hydrogen-Bridged Radical Cations and Ion–Dipole Complexes in The 8th ISMAS Symposium on Mass Spectrometry, Hyderabad, India, 1999, Vol. 1, p. 421.

[13] (a) S.G. Lias, J.E. Bartmess, J.F. Liebman, J.L. Holmes, R.O. Levin, W.G. Mallard, J. Phys. Chem. Ref. Data 17 (1988) Suppl. 1; (b) S.G. Lias, E.P.L. Hunter, ibid. 27 (1998) No 3; (c) C.E.C.A. Hop, P.J.A. Ruttink, G. Schaftenaar, J.K. Terlouw, Chem. Phys. Lett. 156 (1989) 251.

[14] From $\Delta H_f[C_6H_5CN]^{\cdot +} = 274$ kcal/mol [13a], $\Delta H_f[C_6H_5CN] = 52$ kcal/mol [13a], $\Delta H_f[C_6H_5CNH]^+ = 222$ kcal/mol [13a], and $\Delta H_f[C_6H_4CN]^{\cdot} = 111$ kcal/mol; the latter value was obtained using the benzene C–H bond dissociation energy of 111 kcal/mol [13a] and $\Delta H_f[H]^{\cdot} = 52$ kcal/mol [13a].

[15] The CRC Handbook of Chemistry and Physics, R.C. Weast (Ed.), CRC Press, Cleveland, OH, 1974, p. E-64.

[16] Using $\Delta H_f[CH_3C(=O)NH_2]^{\cdot +} = 165$ kcal/mol [13a], $\Delta H_f[CH_3C(=O)NH_2] = -57$ kcal/mol [11a], $\Delta H_f[CH_3C(OH)NH_2]^+ = 103$ kcal/mol [13a] and the values given in [14].

[17] G.A. McGibbon, P.C. Burgers, J.K. Terlouw, Int. J. Mass Spectrom. Ion Processes 191 (1994) 191.

[18] For a recent review see: N. Goldberg and H. Schwarz, Acc. Chem. Res. 27 (1994) 34.

[19] M.A. Trikoupis, P.C. Burgers, P.J.A. Ruttink, J.K. Terlouw, unpublished results.

[20] P.C. Burgers, G.A. McGibbon, J.K. Terlouw, Eur. Mass. Spectrom. 1 (1995) 261.

[21] From $\Sigma\Delta H_f[CH_3C(OH)NH_2^+ + C_6H_4CN^{\cdot}] = 214$ kcal/mol ([13a,14]) and $\Sigma\Delta H_f[C_6H_5CNH^+ + {}^{\cdot}CH_2C(=O)NH_2] = 212$ kcal/mol ([13a], Table 1).

[22] P.J.A. Ruttink, P.C. Burgers, Org. Mass Spectrom. 20 (1993) 1087.

[23] H.B. Schlegel, J. Phys. Chem. 28 (1988) 371.

[24] M. Meot-Ner (Mautner), J. Am. Chem. Soc. 106 (1984) 1257.